

Core-Shell Nanowire Optical Antennas Fed by Slab Waveguides

Jingjing Li, *Student Member, IEEE*, and Nader Engheta, *Fellow, IEEE*

Abstract—A method of realizing nanoantenna systems at optical frequencies is suggested wherein a plasmonic nanowire is placed near a slab waveguide operating near the plasmonic resonant frequency of the nanowire. The polarizability of a nano-sized concentric cylindrical structure with the core made of an ordinary dielectrics and the shell made of a plasmonic material is calculated using Mie scattering theory. When such a core-shell nanowire is placed near a slab waveguide, the transverse magnetic (TM) surface wave guided by the waveguide can interact with the nanowire, and thus part of its energy is scattered into the open space. By reciprocity, under TM wave incidence, the induced dipole on the nanowire will launch a guided mode in the slab waveguide, thus converting part of the incident energy into the guided mode energy. A rigorous analytical treatment of the problem using the Green function of a dipole near a planar slab waveguide is developed, and the properties of such an optical antenna system are studied in detail. The finite element method is also utilized to demonstrate the idea directly.

Index Terms—Antenna feeds, antenna theory, plasmons, scattering.

I. INTRODUCTION

PLASMONIC materials and their electromagnetic properties have been the subject of extensive study in recent years (for some recent review articles see [1]–[4]. Various elements such as plasmonic waveguides [5], [6], optical nanoantennas [7], super lenses [8], [9], deep subwavelength size resonators [10] and nanocircuit elements [11], [12] to name a few, have been studied recently. State-of-the-art nanotechnology provides various fabrication techniques for a wide range of structures including nanowires, nanorods, nanospheres, and nanoshells [13]–[19]. Scattering resonance of plasmonic particles has been well known for a long time. From Mie’s scattering theory, a particle at plasmonic resonance may behave like an induced dipole whose polarizability is determined by the geometry and the material parameters. The polarizability can be very high even though the particle is of deep subwavelength size. It is suggested recently that nanoparticles of concentric structures with cores made of ordinary dielectrics and shell of plasmonic materials, or vice versa, can have resonant frequencies tuned by the ratio of radii of the core and shell in a wide frequency range [13], [14], [20].

Manuscript received August 1, 2006; revised January 15, 2007. This work was supported in part by the U.S. Air Force Office of Scientific Research (AFOSR) under Grant FA9550-05-1-0442

The authors are with the Department of Electrical and Systems Engineering, School of Engineering and Applied Science, University of Pennsylvania, Philadelphia, PA 19104-6390 USA (e-mail: jingjing@seas.upenn.edu).

Color versions of one or more of the figures in this paper are available online at <http://ieeexplore.ieee.org>.

Digital Object Identifier 10.1109/TAP.2007.908534

One of the possible applications of plasmonic materials is to build antenna devices radiating and receiving electromagnetic energy at optical frequencies. There have been growing interests in the concept of antenna devices working at optical frequencies in recent years [7], [11], [21]–[25]. Design and fabrication of optical antennas with prescribed spatial patterns is an interesting and challenging task. One of the main challenges here is the fact that in optical frequencies metals do not usually exhibit high conductivities as in RF and microwaves, but rather, they have permittivities with negative real parts. Therefore, conventional techniques of designing the radiating elements and the waveguides based on the metal properties may be less applicable at optical frequencies, while plasmonic resonance phenomena are often used in optical antenna design. Even though the properties of the materials used for antenna design in the RF (metal) and in the optical (plasmonics) domains are different, the nanoantenna design in the optical regime can benefit from the antenna design experiences in RF and microwave. For example, a half-wavelength dipole antenna was designed and fabricated by Muhlschlegel *et al.* in [7] using noble metals. In another theoretical study, subwavelength particles at plasmonic scattering resonance were suggested as antenna elements and as Yagi–Uda antennas at optical frequencies [11], [24], [25].

In a conventional antenna system in radio frequencies (RF) and microwaves, the source or the load is connected to the antenna through a transmission line or a waveguide, which transfers energy between the two parts. Thus a realistic antenna system is always designed together with the feeding mechanism. However, to the best of our knowledge, most of the current works on optical antennas have dealt with the radiating elements itself, with less attention to the feeding strategy or the complete realization of an optical antenna system including the feeding devices. In this paper, we present, theoretically and numerically, a possible approach for optical antenna systems with the feeding mechanism. Properties of the system such as the energy transfer characteristics and the radiation patterns are given. Finite element method (FEM) is also used to provide numerical simulations.

II. PLASMONIC NANOANTENNA WITH A SURFACE WAVEGUIDE AS A FEEDING MECHANISM

Consider a slab waveguide supporting a guided mode. The field distribution outside of the slab waveguide decays evanescently from the surface. A subwavelength size plasmonic particle is placed near the surface of the waveguide. The particle is of concentric (or coaxial) structure, with the core made of an ordinary dielectrics and shell made of a plasmonic material, and the ratio of radii r_2/r_1 is tuned to make the particle having plasmonic resonance at the frequency of the guided mode. The

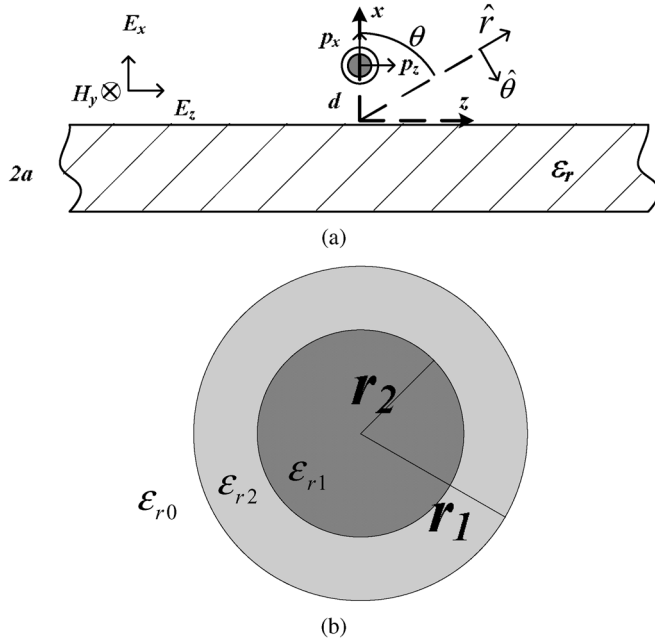


Fig. 1. Schematics of the system. (a) An optical nanoantenna system composed of a core-shell plasmonic nanowire and a slab waveguide. (b) The cross section of the nanowire.

evanescent tail of the surface wave can be scattered by the particle and thus part of its energy can be distributed to the open space. As mentioned before, such a particle can be described as an induced dipole, and the scattering is due to the radiation from the induced dipole in the presence of the slab waveguide. Since the particle is at plasmonic resonance, the polarizability can be large, thus the magnitude of the induced dipole can be of high value and the scattered energy can be a considerable portion of the input energy. By reciprocity, such a system can also work as a receiving device. The incident wave generates an induced dipole on the particle, which will launch a guided mode in the slab waveguide. Due to such a coupling between the nanowire and the slab waveguide, part of the energy carried by the plane wave may be transferred into the guided modes and transported away by the slab waveguide. In this arrangement, the slab waveguide and the plasmonic particle actually form a complete nanoantenna system with the radiating and the feeding elements operating at optical frequencies.¹

For mathematical simplicity, in the following discussions we consider the 2-D version of the problem, that is, a core-shell cylindrical nanowire placed near a planar dielectric waveguide, as shown in Fig. 1(a). Unless otherwise mentioned, the system studied in this paper has the following features: The nanowire has its core made of an ordinary dielectrics (SiO₂) but shell of an-negative plasmonic material (Silver) and is treated as an infinitely long cylinder [see the cross section in Fig. 1(b)]. Under a TM-polarized incident wave (for which the only component

¹For the sake of simplicity in the analysis, here we assume that this nanoparticle (or nanowire, as we assume later) is located above the top surface of the waveguide with a distance d from the surface, suspended in free space with permittivity ϵ_0 and permeability μ_0 . In a more practical scenario, a thin layer of dielectric will have to be placed between the waveguide and the nanoparticle, so that the particle can be printed on this thin dielectric. The presence of such a thin layer may not significantly affect the main conclusions discussed in this paper.

of the magnetic field is parallel to the nanowire axis), the scattered field of the nanowire is dominated by the two-dimensional (2-D) dipolar term at plasmonic resonance. It is worth clarifying that the “dipole” here (and through out this paper) takes the meaning in a 2-D problem, i.e., a 2-D dipole of magnitude p is an infinitely long line extending along the third dimension with dipoles sitting on it uniformly so that on an infinitesimal segment of length δl there exists a dipole of magnitude $p\delta l$. Thus a dipole in 2-D actually has the unit of the charge. At the operating frequency the free-space wavelength is 550 nm at which the relative permittivity of silver is $\epsilon_{r1} = -11.046 - 0.337j$ [26] and $\epsilon_{r2} = 2.2$ for SiO₂. The ratio of radii (r_2/r_1) for the nanowire is set to the value at which the nanowire is at its scattering resonance at 550 nm (the calculation is briefly discussed in the next section). The outer radius of the nanowire is $r_1 = 0.05\lambda_0 = 27.5$ nm. The waveguide has a relative permittivity of ϵ_r and can be made of conventional dielectrics or plasmonic materials (e.g., Ag, Au), but in this paper we concentrate most of our discussions on systems using a slab waveguide of $\epsilon_r = 4.0$ (such as quartz crystal). When the setup is used as a transmitting antenna, a guided TM mode as

$$\begin{aligned} H_y &= H_0 \cos(k_x(x+a)) e^{-jk_z z} & -2a < x < 0 \\ H_y &= H_0 \cos(k_x a) e^{-\alpha_x x} e^{-jk_z z} & x < 0 \end{aligned} \quad (1)$$

is fed from the left end of the waveguide [the origin of the coordinate system is at the surface of the waveguide, see Fig. 1(a)]. Here H_0 is the magnitude of the magnetic field at the center of the waveguide and k_z is the propagating constant of the guided mode along \hat{z} direction. $\alpha_x^2 = k_z^2 - k_0^2$ and $k_x^2 = \epsilon_r k_0^2 - k_z^2$. When used as a receiving antenna, a plane wave with the TM polarization (i.e., its magnetic field parallel with the \hat{y} axis) is incident on this system with an incidence angle θ (with respect to the \hat{x} axis) as

$$H_y = H_0 e^{j(k_0 x \cos \theta + k_0 z \sin \theta)}. \quad (2)$$

III. SCATTERING OF A CYLINDRICAL NANOWIRE PLACED NEAR SURFACE WAVEGUIDE

The key issue in studying this antenna system is to calculate the induced dipole on the nanowire under certain input fields. In the transmit mode, the applied input field is the field of a guided mode carried by the slab waveguide as in (1), while in the receive mode the input is an incident plane wave described in (2). Following a similar approach to the Mie theory [20], [27], [28] it can be shown that under TM incidence (i.e., the only magnetic component is parallel with the nanowire’s axis), a nanowire of subwavelength radius as shown in Fig. 1(b) behaves like a 2-D induced “dipole” line (hereafter we simply call it a dipole), with the polarizability α as

$$\alpha = \frac{8j c_1 \epsilon_0}{k_0^2} \quad (3)$$

where c_1 is the scattering coefficient of the dipolar term given as

$$c_1 = -\frac{U_1}{U_1 - jV_1} \quad (4)$$

with

$$U_1 = \begin{pmatrix} \frac{J_1(k_1 r_2)}{k_1} & \frac{J_1(k_2 r_2)}{k_2} & \frac{Y_1(k_2 r_2)}{k_2} & 0 \\ \frac{J_1'(k_1 r_2)}{k_1} & \frac{J_1'(k_2 r_2)}{k_2} & \frac{Y_1'(k_2 r_2)}{k_2} & 0 \\ 0 & \frac{J_1(k_2 r_1)}{k_2} & \frac{Y_1(k_2 r_1)}{k_2} & \frac{J_1(k_0 r_1)}{k_0} \\ 0 & \frac{J_1'(k_2 r_1)}{k_2} & \frac{Y_1'(k_2 r_1)}{k_2} & \frac{J_1'(k_0 r_1)}{k_0} \end{pmatrix} \quad (5a)$$

$$V_1 = \begin{pmatrix} \frac{J_1(k_1 r_2)}{k_1} & \frac{J_1(k_2 r_2)}{k_2} & \frac{Y_1(k_2 r_2)}{k_2} & 0 \\ \frac{J_1'(k_1 r_2)}{k_1} & \frac{J_1'(k_2 r_2)}{k_2} & \frac{Y_1'(k_2 r_2)}{k_2} & 0 \\ 0 & \frac{J_1(k_2 r_1)}{k_2} & \frac{Y_1(k_2 r_1)}{k_2} & \frac{Y_1(k_0 r_1)}{k_0} \\ 0 & \frac{J_1'(k_2 r_1)}{k_2} & \frac{Y_1'(k_2 r_1)}{k_2} & \frac{Y_1'(k_0 r_1)}{k_0} \end{pmatrix} \quad (5b)$$

$J_1(x)$ and $Y_1(x)$ are the first and second kind Bessel functions of order 1. It is straightforward to confirm that for the materials used here, the nanowire achieves the scattering resonance at the working wavelength of 550 nm when $r_2/r_1 = 0.732$. Under input electric field E_i , the induced dipole of the nanowire can be written as

$$\mathbf{p} = \alpha \mathbf{E}_{\text{loc}} = \alpha \left(\mathbf{E}_i^{(w)} + \mathbf{E}_s^{(w)} \right) \quad (6)$$

where \mathbf{E}_{loc} is the local field that is composed of the input field (\mathbf{E}_i), and the part of the dipole radiation scattered by the waveguide (\mathbf{E}_s). The superscript “(w)” denotes the value of the field evaluated at the position of the nanowire. \mathbf{E}_s can be expressed in terms of the dyadic Green’s function as

$$\begin{aligned} \mathbf{E}_s &= \int \left(\bar{\bar{G}}_1(\mathbf{r}, \mathbf{r}') - \bar{\bar{G}}_0(\mathbf{r}, \mathbf{r}') \right) \cdot \mathbf{J}(\mathbf{r}') dV \\ &= \int \left(\bar{\bar{G}}_1(\mathbf{r}, \mathbf{r}') - \bar{\bar{G}}_0(\mathbf{r}, \mathbf{r}') \right) \cdot j\omega \mathbf{p} \delta(w) dV \\ &= \bar{\bar{G}}^{(w)} \cdot \mathbf{p} \end{aligned} \quad (7)$$

where $\bar{\bar{G}}_1$ is the dyadic green function of the slab waveguide while $\bar{\bar{G}}_0$ is that of the free space. $\bar{\bar{G}} = j\omega \left(\bar{\bar{G}}_1 - \bar{\bar{G}}_0 \right)$ and again $\bar{\bar{G}}^{(w)}$ means the value of $\bar{\bar{G}}$ at the position of the nanowire. $\bar{\bar{G}}$ is actually the scattered part in Green’s function. Combining (6) and (7) we can express the induced dipole directly in terms of the incident electric field as

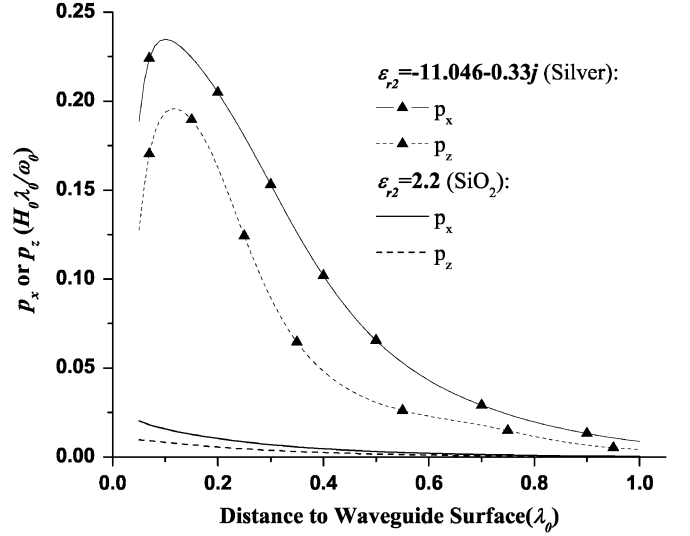
$$\mathbf{p} = \left(\mathbf{I} - \alpha \bar{\bar{G}}^{(w)} \right)^{-1} \alpha \mathbf{E}_i^{(w)} \quad (8)$$

Since α is known, the induced dipole can be obtained for any incident field when one has $\bar{\bar{G}}^{(w)}$. The problem of dyadic Green’s function near a dielectric slab has been studied extensively in the past (see, e.g., [29] and [30]). Following the approach described in [29], the results show that

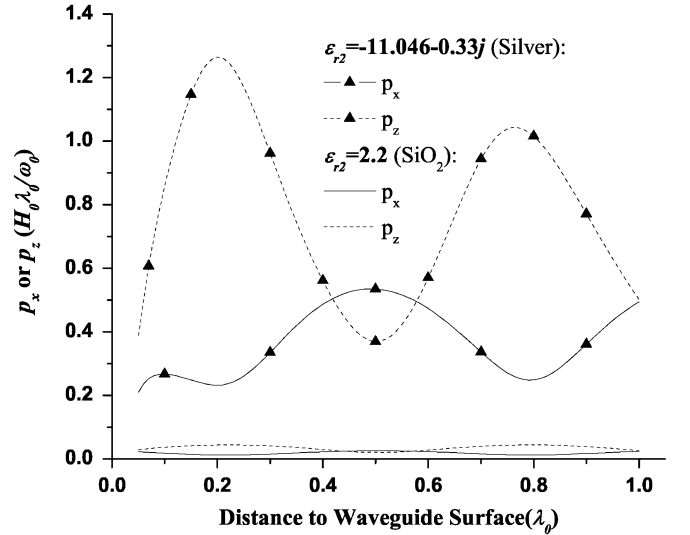
$$\bar{\bar{G}} = \begin{pmatrix} g_{xx} & 0 \\ 0 & g_{zz} \end{pmatrix} \quad (9)$$

with

$$\begin{aligned} g_{xx} &= \frac{1}{4\pi\epsilon_0} \int_c k_z^2 \frac{\text{Re}^{-\alpha_x(x+d)}}{\alpha_x} e^{-jk_z z} dk_z \\ g_{zz} &= -\frac{1}{4\pi\epsilon_0} \int_c \alpha_x R e^{-\alpha_x(x+d)} e^{-jk_z z} dk_z \end{aligned} \quad (10)$$



(a)



(b)

Fig. 2. Magnitude of the induced dipole versus the distance between the center of the nanowire and the surface of the slab waveguide, under the (a) transmit mode and (b) receive mode. The case of the core-shell plasmonic nanowire (lines with triangle marks, $\epsilon_{r1} = 2.2$, $\epsilon_{r2} = -11.046 - 0.337j$) and the single-material nonplasmonic dielectric nanowire (lines with no triangle marks, $\epsilon_{r1} = \epsilon_{r2} = 2.2$) are considered. Both nanowire has an outer radius $r_1 = 0.05\lambda_0$.

where d is the distance from the center of the nanowire to the surface of the waveguide, and R is the reflection coefficient of the waveguide defined as

$$R = \frac{1}{2} \left(\frac{\alpha_x \epsilon_r + k_x \tan k_x a}{\alpha_x \epsilon_r - k_x \tan k_x a} + \frac{\alpha_x \epsilon_r - k_x \cot k_x a}{\alpha_x \epsilon_r + k_x \cot k_x a} \right) \quad (11)$$

where (10) can be evaluated numerically for our problem, and the induced dipole moment can then be obtained.

Fig. 2 presents the magnitudes of the components of induced dipole \mathbf{p} in terms of the separation of the nanowire from the slab (d), under both the transmit mode [in Fig. 2(a)] and the receive mode [in Fig. 2(b)]. When the setup is used as a transmitting antenna, a TM guided mode described as (1) is considered as the “input” wave and $E_i^{(w)}$ is the electric field of

this mode evaluated at the position of the nanowire. The magnitude of the induced dipole is shown in Fig. 2(a) as the lines with triangle marks. One of the interesting features of the variation of p_l ($l = x$ or z) versus d , is that, $|p_l|$ does not decay in the same manner as the exponentially decaying magnitude of E_i away from the slab surface. Instead, the maximum of $|p_l|$ occurs at a certain distance from the surface. This is mainly due to the effect of the interference between the dipole field, and the scattered field of the dipole from the slab. In other words, p_l has a local maximum when $|\alpha(1 - \alpha g_u)^{-1} e^{-\alpha_x d}|$, $l = x, z$ is locally maximized. Similar interference effect has also been observed in the fluorescence of single molecules placed near a planar structure [31]. When the antenna is working under the receive mode, the results are shown in Fig. 2(b) as lines with triangle marks, for which a TM plane wave described in (2) is incident on this structure. In this plot we use $\theta = 30^\circ$. In this case $E_i(w)$ denotes the sum of the electric field of the plane wave and the reflection of this plane wave from the slab waveguide when nanowire is absence. Again due to the interference between the incident and reflected field, there is an obvious variation of the magnitude of the induced dipole when the distance between nanowire and waveguide varies. For comparison, the induced dipoles for a system using a single-material nonplasmonic dielectric nanowire (for which we use $\epsilon_{r1} = \epsilon_{r2} = 2.2$) under both the transmit and receive modes are also plotted in Fig. 2(a) and (b) (the lines with no triangle marks). We also note that, as expected, the induced dipole is much stronger for the concentric core-shell plasmonic nanowire than the single-material nonplasmonic dielectric nanowire, because the polarizability of the former is much higher. This is in general true for single-material nanowires of different positive permittivity. In fact, nanowires of high-positive-value permittivity do provide higher polarizability. However, they can hardly compete with the plasmonic nanowires. The induced dipoles of conventional nanowires are of the same order of magnitude even for nanowires of relative permittivity as high as 20.

IV. PROPERTIES OF THE CORE-SHELL NANOWIRE OPTICAL ANTENNA FED BY THE SLAB WAVEGUIDE

From a knowledge of induced dipole moments on the nanowire, we can now study the transmitting and receiving properties of such optical antenna systems in details. We now consider several aspects of the performance of such a nanoantenna.

A. Radiation Patterns

The value of the field at any position can be evaluated following an approach similar to that in [29], and the asymptotic behavior of the electric field in the far zone can be evaluated using the conventional steepest decent contour (SDC) method after a transformation of $k_z = k_0 \sin \phi$ where ϕ is generally complex. The far-zone radiated electric field can be written as

$$E_\theta = j \frac{\sqrt{2} k_0^2}{4\pi \epsilon_0} e^{-j(k_0 r - \pi/4)} \left(\frac{1}{k_0 r} \right)^{1/2} \times (\sqrt{\pi} e^{j k_0 d \cos \theta} + R(\theta) \Gamma(1/2) e^{-j k_0 d \cos \theta}) \times (p_x \sin \theta - p_z \cos \theta) \quad (12)$$

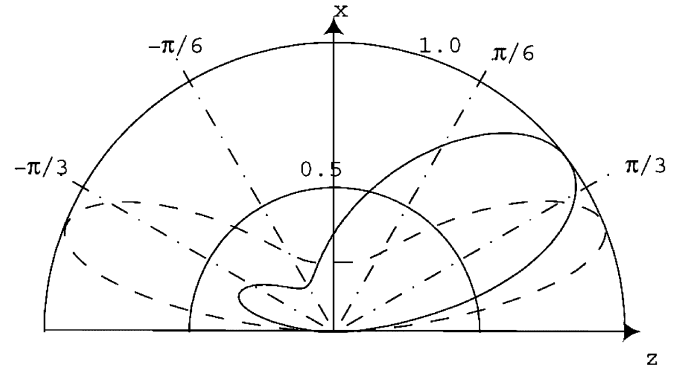


Fig. 3. Calculated radiation patterns. Solid: $d = 0.100\lambda_0$. Dash: $d = 0.195\lambda_0$.

where θ is the angle measured from the \hat{x} axis [refer to Fig. 1(a)], $R(\theta)$ is the reflection coefficient evaluated from (11) at $k_z = k_0 \sin \theta$ and corresponding k_x and α_x .

Fig. 3 shows the radiation patterns of this nanoantenna for the cases of $d = 0.100\lambda_0$ (solid line) and $d = 0.195\lambda_0$ (dashed line). In each case, the pattern is normalized to its own maximum value. Since the two components of the induced dipole (p_x and p_z) is connected to E_i through $\bar{\bar{G}}^{(w)}$ by (8) and (9), while the components of $\bar{\bar{G}}^{(w)}$ is determined by d as in (10), the relative magnitude and phase of p_x with respect to p_z is different at different d . Thus the pattern has different forms at different d . For the case of $d = 0.100\lambda_0$, the pattern has a forward-going main lobe (relative to the direction of incident guided mode) at around 50° , and a smaller backward-going side lobe at around -65° . When $d = 0.195\lambda_0$, however, the pattern is almost symmetric with the lobes directed at around $\pm 65^\circ$.

B. Power Transfer

One of the key characteristics of an antenna system is the ability to transfer the input energy into the radiated energy. The power transfer properties of the system when used as a transmitting antenna is shown in Fig. 4. Under the transmit mode, the input guided mode energy can be considered as the “input” energy P_{in} . The radiated power density can be calculated as $|E_\theta|^2/\eta_0$ where E_θ is defined as (12) and η_0 is the intrinsic impedance of the free space. Thus the total radiated power P_{rad} is an integration of $|E_\theta|^2/\eta_0$ over the region of $-\pi/2 < \theta < \pi/2$, i.e., the region above the slab waveguide. The normalized total radiated energy P_{rad}/P_{in} , is shown in Fig. 4 as the solid line with open triangles. When the distance between the nanowire and the waveguide becomes large, the coupling between the nanowire and the waveguide decreases, as expected, and thus P_{rad} approaches zero. However, P_{rad} does not increase monotonically as d decreases, due to the interference effect discussed before. The maximum of P_{rad} happens at around $d = 0.09\lambda_0$ and the maximum of P_{rad}/P_{inc} can get to 14.2%. The induced dipole also launches guided modes that can propagate in the positive and negative \hat{z} directions in the waveguide. For a dipole \mathbf{p} with components p_x and p_z , the launched guided mode

with propagating constant k_z has the magnetic field distribution outside of the waveguide ($x > 0$) as

$$H_{k_z} = \mp \frac{\omega}{2} \frac{e^{-\alpha_x d}}{\alpha_x} F(k_z) (k_z p_x + j \alpha_x p_z) e^{-\alpha_x x} e^{-j k_z z} \quad (13)$$

with sign for $k_z > 0$ (propagating to the $+z$ direction) and $+$ sign for $k_z < 0$ (propagating to the $-z$ direction). $F(k_z)$ is the residue of the reflection coefficient R (11) at k_z . The guided mode launched by the induced dipole that propagates in the negative z direction is actually the reflection from the waveguide-antenna interface, and the ratio of the energy carried by the reflected guided mode to the input energy ($P_{\text{ref}}/P_{\text{in}}$) is shown as the solid line with stars in Fig. 4. The guided mode propagating in the $+\hat{z}$ direction, when added to the original input guided mode (1), gives the transmitted guided mode leaving the waveguide-antenna interface and propagating to the right end of the slab waveguide. The ratio of the energy carried by the transmitted guided mode to the input energy ($P_{\text{tra}}/P_{\text{in}}$) is shown as the solid line with solid triangles in Fig. 4. The reflected and transmitted energies are not radiated away, but are important figures of merits of the system. Note that the sum of the radiated, reflected and transmitted energies does not add up to the input energy, since there is still some energy that is radiated to the other side of the slab waveguide, which is not of interest here and is not calculated. As the nanowire-waveguide distance d increases to a large value, the coupling between the nanowire and the waveguide becomes weak, so that little energy will reflect back (shown in the plot that $P_{\text{ref}}/P_{\text{in}}$ approaches 0), most of the input energy will transmit to the right side of the waveguide ($P_{\text{tra}}/P_{\text{in}}$ approaches 1), as expected. But again, maximum reflection and minimum transmission happens at some certain d due to the interference. The gain of the antenna, defined as the ratio of the radiation intensity at the maximum direction to the radiation intensity that would be obtained if all the incident power were radiated isotropically in the upper half-space $-\pi/2 < \theta < \pi/2$, is shown in Fig. 5. The maximum of the gain is about 0.346 and happens when $d \sim 0.076\lambda_0$.

The energy transfer property when the system is working as a receiving antenna is also calculated for incident angle $\theta = 30^\circ$. As described before, the induced dipole launches guided modes that carry energy transferred from the incident wave. The guided modes propagate to both directions and can be collected at either end of the waveguide as the received energy of the antenna. When divided by the incident power density, it gives the effective receiving cross section of the antenna (in unit of λ_0), which is shown in Fig. 6. Both the $-z$ -end receiving and the $+z$ -end receiving situations are shown in the plot. Notice that as d varies, the maximum of the receiving cross section is $\sim 0.31\lambda_0$ for the incident angle $\theta = 30^\circ$ even though the radius of the nanowire is only $0.05\lambda_0$.

For the purpose of comparison, the properties of a system using a single-material nonplasmonic dielectric nanowire made of SiO_2 of the same size as the antenna element is also calculated. These properties are shown as the dashed lines in Figs. 4 and 6. For this system, the maximum of $P_{\text{rad}}/P_{\text{inc}}$ (the dashed line with open triangles in Fig. 4) is in order of 10^{-4} , several orders smaller than that of a system using plasmonic nanowire. $P_{\text{ref}}/P_{\text{in}}$ (dashed line with stars in Fig. 4) is almost 0 while

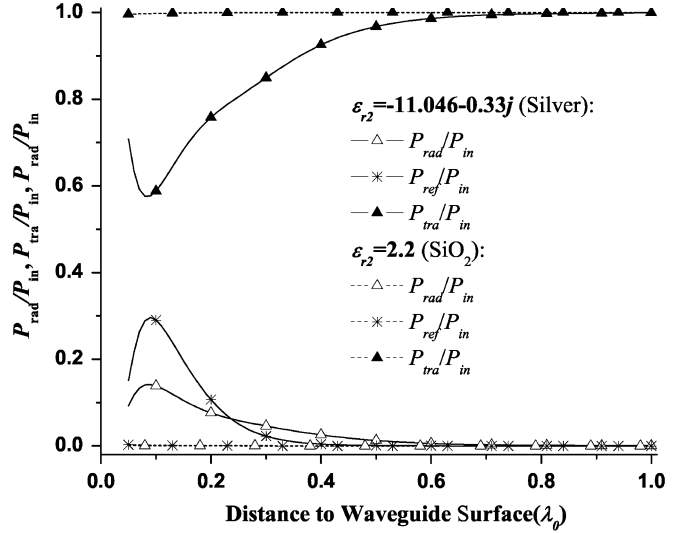


Fig. 4. Power transfer properties under the transmit configuration: the radiated, reflected and transmitted power. For antenna systems using a core-shell plasmonic nanowire (solid lines) or using a single-material nonplasmonic dielectric nanowire (dashed lines).

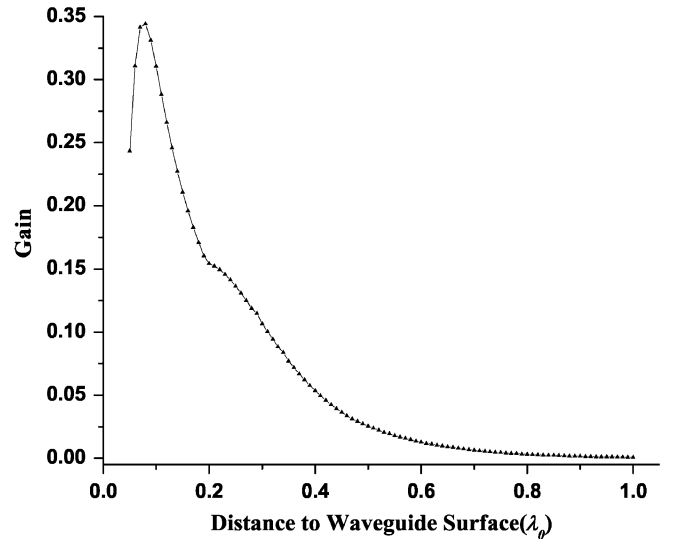


Fig. 5. Gain of the antenna system versus d .

$P_{\text{tra}}/P_{\text{in}}$ (dashed line with solid triangles in Fig. 4) is almost 1 for any d , which means most of the energy is transmitted to the right of the waveguide, and little reflected back. In other words, the existence of the nanowire made of ordinary dielectrics has little influence on the mode propagation of the waveguide. The receiving cross section of such a system is shown in Fig. 6 as dashed lines. The cross section when receiving at $-z$ direction (dashed line with stars in Fig. 6) or at $+z$ direction (dashed line with open squares in Fig. 6) are both orders of magnitude smaller than those of the plasmonic nanowire at any given d .

C. Dispersion Characteristics

In order to analyze the frequency dependence of the radiation characteristics of our nanoantenna system, we need to take into account the frequency dispersion of the plasmonic material. A Drude model is used to describe the frequency dependence

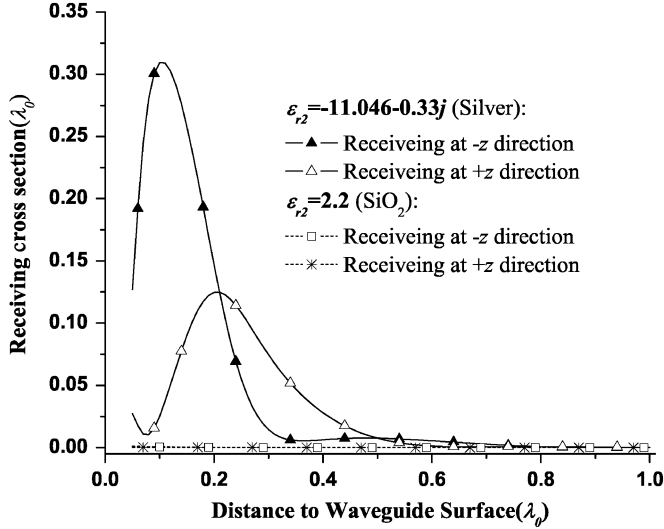


Fig. 6. Receiving cross section of the systems, with a core-shell plasmonic nanowire or the single-material nonplasmonic dielectric nanowire.

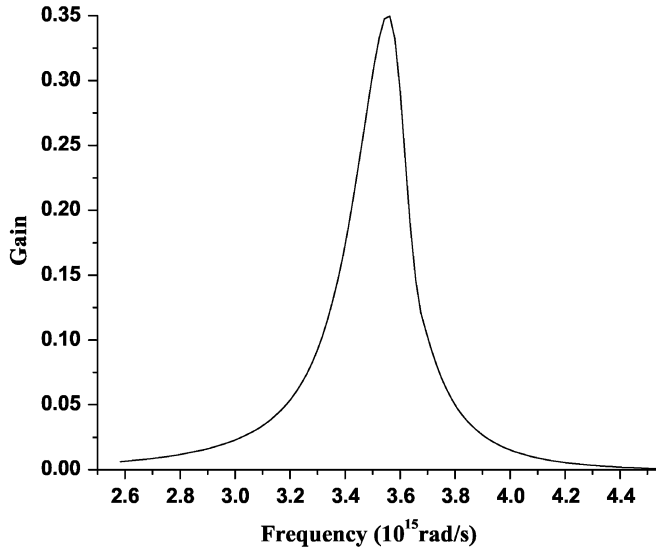


Fig. 7. Gain versus frequency. The nanowire has $\epsilon_{r1} = 2.2$, $b/a = 0.732$, $r_1 = 55$ nm and ϵ_{r2} follows (14).

of the permittivity of silver which is the shell material in the nanowire, i.e.

$$\epsilon_r(\omega) = 1 - \frac{\omega_p^2}{\omega(\omega - j\Gamma_c)} \quad (14)$$

where ω_p is the plasma frequency and Γ_c the collision frequency. The numerical values of ω_p and Γ_c are obtained by fitting the Drude model to the available experimental results for permittivity of silver [26] in the visible domain. They are expressed as $\omega_p = 1.23 \times 10^{16}$ and $\Gamma_c = 7.90 \times 10^{13}$ (rad/s). Fig. 7 presents the plot of the gain of the system over the range of visible domain when $d = 55$ nm. The center frequency where the maximum gain occurs actually corresponds to $\lambda_0 = 530$ nm, shifted a little from the scattering resonant frequency of the nanowire for which $\lambda_0 = 550$ nm. This is because the gain is determined by both the polarizability and the

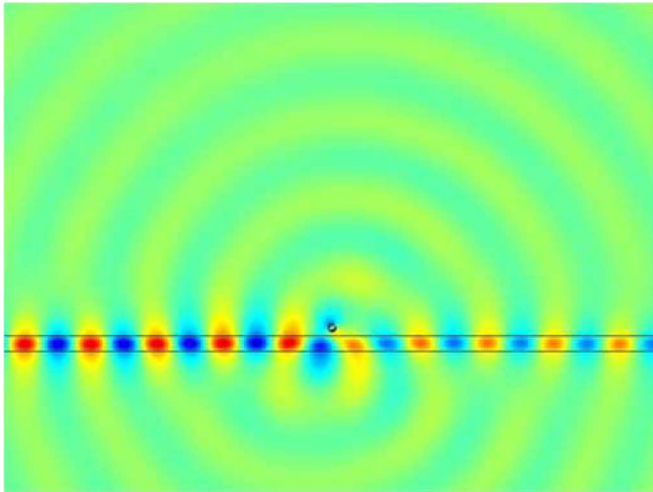
nanowire-waveguide separation distance (d), and the relative distance d/λ_0 changes with the frequency. The bandwidth of our antenna can also be estimated from this plot by finding the full-width-half-maximum (FWHM) of the gain distribution. The quality factor Q can then be evaluated as $Q = f_0/\text{FWHM}$ where f_0 is the center frequency. Since the radiator is electrically small (in the $x - z$ plane, $r_1 = 27.5$ nm, while the center frequency corresponds to $\lambda_0 = 530$ nm), one may expect a high Q , thus a very small bandwidth for this system. However, our calculations show that the bandwidth is relatively broad with $\text{BW} = 3.82 \times 10^{13}$ (rad/s) and $Q = 14.8$. This is mainly due to the fact that our radiating system is actually composed of the nanowire and the surface waveguide which is ideally infinitely large. The material loss also helps broaden the bandwidth.

V. FINITE ELEMENT METHOD (FEM) SIMULATIONS

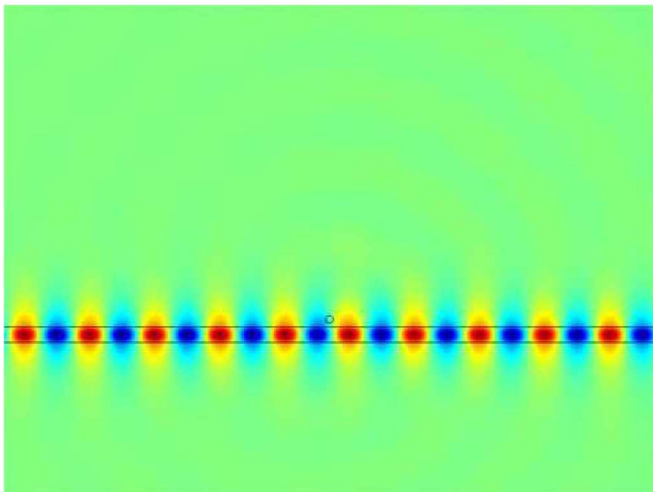
Using the commercially available FEM software COMSOL Multiphysics, we simulate our set up in the transmit (Fig. 8) and the receive (Fig. 9) modes. In these figures, the “rectangle” is the cross section of the planar slab waveguide, while the small circle is the nanowire. Here, we take the concentric core-shell plasmonic nanowire at $d = 0.1\lambda_0$. In Fig. 8(a), the incident guided mode is launched from the left entrance of the waveguide. The plot shows the instantaneous distribution of the magnetic field. We see that due to the core-shell nanowire, the scattered wave is present in the form of ring-like distribution centered at the nanowire. This field distribution actually propagates away, as can be seen by checking the results at different phase angle. We note that the guided mode in the waveguide in the right side of the nanowire is much weaker than the input, implying $P_{\text{tra}}/P_{\text{in}}$ to be small. This is another indication of the effect of the nanowire. For comparison, Fig. 8(b) shows the instantaneous magnetic field in the same set up when a single-material nonplasmonic nanowire of the same radius but of positive relative permittivity is used. Since the polarizability of positive-permittivity nanowire increases with the magnitude of the relative permittivity, a relatively large value of 20 is used to highlight the possible effects. The color scale is set to the same as Fig. 8(a). As can be seen in the picture, the radiation from the positive-permittivity nanowire is essentially not noticeable, even though a high-permittivity nanowire is used.

Simulation results of the system in the receive mode are shown in Fig. 9, in (a) the core-shell plasmonic nanowire is used while in (b), a single-material nonplasmonic nanowire of relative permittivity of 20 is used. A TM-polarized plane wave is incident from the top and again the plot is the instantaneous field distribution of the magnetic field. The nodes inside the waveguide in Fig. 9(a) actually indicate the guided mode launched by the induced dipole. However, when a single-material nonplasmonic nanowire is used as in Fig. 9(b), almost no guided mode is excited. We do see that the magnitude of the field inside the waveguide is higher than that outside. This effect, which is not a guided propagating mode, is due to the interference of the incident plane wave and the waves scattered from the two waveguide surfaces.

The former discussions concentrated on a system using only one core-shell plasmonic nanowire as the antenna element. Systems using multiple antenna elements can also be analyzed fol-



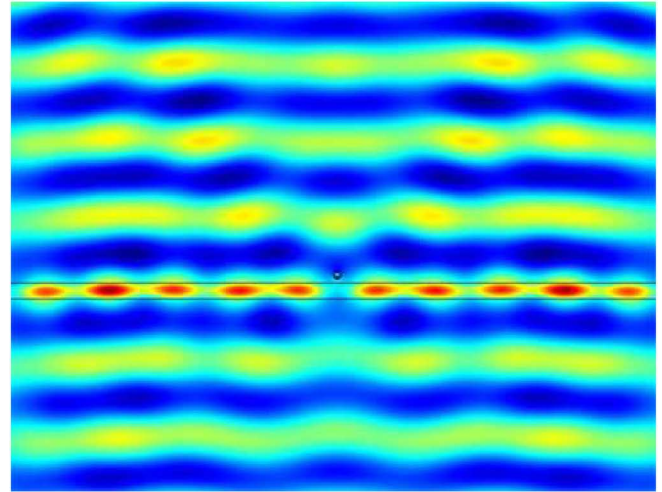
(a)



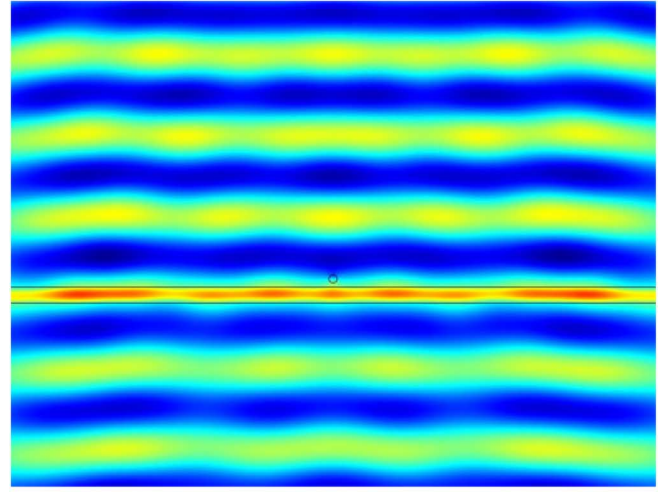
(b)

Fig. 8. Instantaneous magnetic field distribution from the FEM simulation of the system under the transmit mode. Case of (a) core-shell plasmonic nanowire and (b) single-material nonplasmonic nanowire of $\epsilon_r = 20$. In both (a) and (b) the system is fed from the left.

lowing a similar approach by taking into account the coupling between the elements. By properly arranging the positions of the antenna elements, we can design the radiation pattern of the antenna system. Without going into the detailed analysis, here we present some FEM simulation results, as in Fig. 10. In these simulations, three antenna elements are put at the same distance to the surface of the waveguide, but the distances between the neighboring nanowires are different for the two cases. In Fig. 10(a), the distance between each two neighboring elements is λ_g where λ_g is the guided wavelength, thus the input field at the location of each element is of the same phase. The phases of the induced dipoles on each nanowire should be close to each other, so that the maximum radiation direction is expected to be perpendicular to the waveguide. This is actually verified by the results shown in Fig. 10(a). As the distance between the neighboring elements decreases, the phases are no longer equal, but each element has a leading phase compared to the neighboring one at its right side. Thus the beam will be tilted to the right side. This is demonstrated by Fig. 10(b), for which the distance be-



(a)



(b)

Fig. 9. FEM simulation of the receiving property of the system. The waveguide has a thickness of $0.2\lambda_0$ and $\epsilon_r = 4.0$. Case of (a) core-shell plasmonic nanowire and (b) single-material nonplasmonic nanowire of $\epsilon_r = 20$.

tween each two neighboring elements is $\lambda_g/2$, and a maximum radiation at approximately 45° is observed.

In the analysis and simulations up to Fig. 9 we used a slab waveguide made of ordinary dielectrics ($\epsilon_r = 4.0$). We would like to point out that plasmonic materials can also be used to make the waveguide, and the waveguides used in Fig. 10 are actually made of a $\epsilon_r = -2.0$ material (the loss of the plasmonic material for the waveguide is neglected for the sake of simplicity). Notice that the guided mode on this waveguide has the maxima at the interfaces, a specific feature of the plasmonic waveguide. Depending on the applications, plasmonic waveguides can have advantages over the ordinary dielectric waveguides. For example, since the surface mode on plasmonic waveguide is usually more tightly bound, the system can be more compact along the direction perpendicular to the waveguide. Also, under the transmit mode, it is more difficult for the radiated field of the induced dipole to transfer through the plasmonic slab and get into the other side. Thus the radiation of the system can be confined to the upper region, increasing the performance of the system.

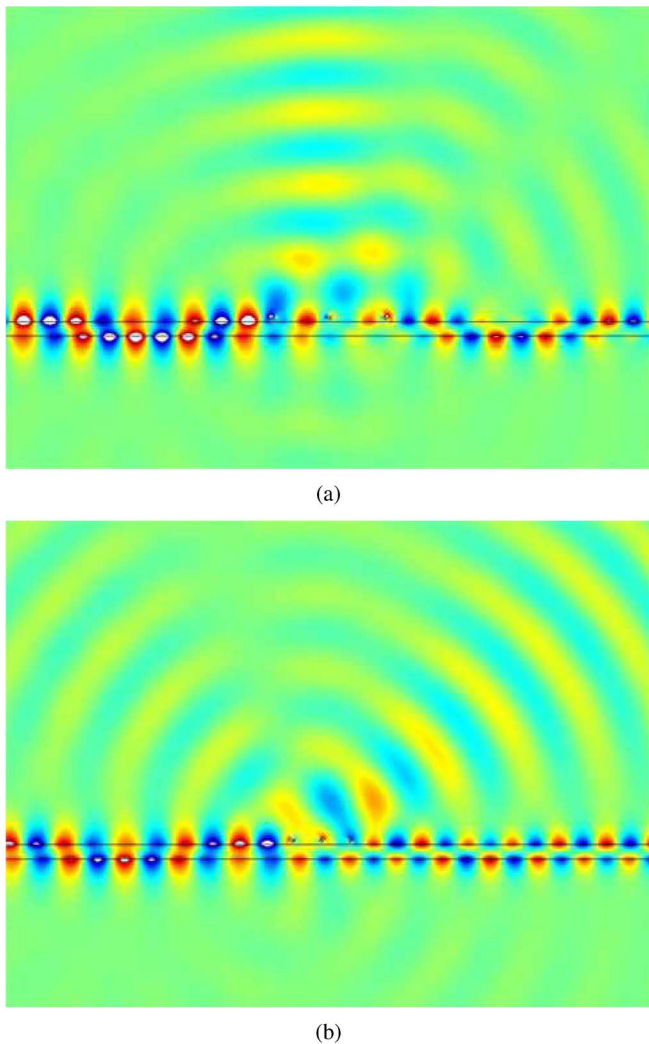


Fig. 10. Antenna systems using multiple nanoantenna elements. (a) Three nanoantenna elements, placed at an equal distance to the surface of the waveguide, and separated with λ_g from each neighboring element. (b) Similar to (a), except the separation between the elements is $\lambda_g/2$. λ_g is the guided wavelength of the guided mode.

VI. SUMMARY

In this paper, we suggested a method of realizing nanoantenna systems with feeding element working at optical frequencies by placing plasmonic subwavelength nanowires near a surface waveguide. The properties of such an antenna system were studied in details using Green's function of a dipole near a slab waveguide. The results showed that a considerable portion of the input optical energy can be radiated out. By using a Drude model of the plasmonic material the dispersion properties of the system were also studied. Finite element method was used to simulate the set up. Using the FEM simulations, we also demonstrated the idea of tailoring the radiation patterns of this optical antenna system by properly placing multiple nanoantenna elements near the feeding slab waveguide.

REFERENCES

- [1] S. I. Bozhevolnyi and V. M. Shalaev, "Nanophotonics with surface plasmons—Part I," *Photonic Spectra*, vol. 40, no. 1, p. 58, 2006.
- [2] S. I. Bozhevolnyi and V. M. Shalaev, "Nanophotonics with surface plasmons—Part II," *Photonic Spectra*, vol. 40, no. 2, p. 66, 2006.
- [3] E. Ozbay, "Plasmonics: Merging photonics and electronics at nanoscale dimensions," *Science*, vol. 311, no. 5758, pp. 189–193, 2006.
- [4] S. A. Maier and H. A. Atwater, "Plasmonics: Localization and guiding of electromagnetic energy in metal/dielectric structures," *J. Appl. Phys.*, vol. 98, p. 011101, 2005.
- [5] L. A. Sweatlock, S. A. Maier, H. A. Atwater, J. J. Penninkhof, and A. Polman, "Highly confined electromagnetic fields in arrays of strongly coupled ag nanoparticles," *Phys. Rev. B.*, vol. 71, p. 235408, 2005.
- [6] V. Podolskiy, A. Sarychev, and V. Shalaev, "Plasmon modes in metal nanowires," *J. Nonlinear Opt. Phys. Mater.*, vol. 11, no. 1, pp. 65–74, 2002.
- [7] P. Muhlschlegel, H. J. Eisler, O. J. F. Martin, B. Hecht, and D. W. Pohl, "Resonant optical antennas," *Science*, vol. 308, pp. 1607–1609, 2005.
- [8] G. Shvets and Y. A. Urzhumov, "Engineering the electromagnetic properties of periodic nanostructures using electrostatic resonances," *Phys. Rev. Lett.*, vol. 93, p. 243902, 2004.
- [9] N. Fang, H. Lee, and X. Zhang, "Sub-diffraction-limited optical imaging with a silver superlens," *Science*, vol. 308, pp. 534–537, 2005.
- [10] J. Li and N. Engheta, "Ultracompact sub-wavelength plasmonic cavity resonator on a nanowire," *Phys. Rev. B.*, vol. 74, p. 115125, 2006.
- [11] N. Engheta, A. Salandrino, and A. Alu, "Nanocircuit elements, nano-transmission lines, and nano-antennas using plasmonic materials in the optical domain," presented at the IEEE Int. Workshop on Antenna Technology: Small Antennas and Novel Metamaterials (iWAT'05), Singapore, Mar. 7–9, 2005.
- [12] N. Engheta, A. Salandrino, and A. Alu, "Circuit elements at optical frequencies: Nanoinductors, nanocapacitors, and nanoresistors," *Phys. Rev. Lett.*, vol. 95, p. 095504, 2005.
- [13] R. D. Averitt, D. Sarkar, and N. J. Halas, "Plasmon resonance shifts of Au-coated Au₂S nanoshells: Insight into multicomponent nanoparticle growth," *Phys. Rev. Lett.*, vol. 78, no. 22, pp. 4217–4220, 1997.
- [14] J. B. Jackson and N. J. Halas, "Silver nanoshells: Variations in morphologies and optical properties," *J. Phys. Chem. B.*, vol. 105, no. 14, pp. 2743–2746, 2001.
- [15] R. L. D. Whitby, W. K. Hsu, Y. Q. Zhu, H. W. Kroto, and D. R. M. Walton, "Novel nanoscale architectures: Coated nanotubes and other nanowires," *Phil. Trans. R. Soc. Lond. A.*, vol. 362, no. 1823, p. 2127C2142, 2004.
- [16] M. Law, J. Goldberger, and P. Yang, "Semiconductor nanowires and nanotubes," *Annu. Rev. Mater. Res.*, vol. 34, pp. 83–122, 2004.
- [17] L. Li, Y.-W. Yang, G.-H. Li, and L.-D. Zhang, "Conversion of a Bi nanowire array to an array of Bi-Bi₂O₃ core-shell nanowires and Bi₂O₃ nanotubes," *Small*, vol. 2, no. 4, pp. 548–553, Apr. 2006.
- [18] A. Borrás, A. Barranco, F. Yubero, and A. R. Gonzalez-Elipe, "Supported Ag-TiO₂ core-shell nanofibres formed at low temperature by plasma deposition," *Nanotechnol.*, vol. 17, no. 14, pp. 3518–3522, Jun. 2006.
- [19] K. Huang, Y. Zhang, Y. Long, J. Yuan, D. Han, Z. Wang, L. Niu, and Z. Chen, "Preparation of highly conductive, self-assembled gold/polyaniline nanocables and polyaniline nanotubes," *Chem. Eur. J.*, vol. 12, no. 20, pp. 5314–5319, July 2006.
- [20] A. Alu and N. Engheta, "Polarizabilities and effective parameters for collections of spherical nanoparticles formed by pairs of concentric double-negative, single-negative, and/or double-positive metamaterial layers," *J. Appl. Phys.*, vol. 97, p. 094310, 2005.
- [21] S. J. Oldenburg, J. B. J. G. D. Hale, and N. J. Halas, "Light scattering from dipole and quadrupole nanoshell antennas," *Appl. Phys. Lett.*, vol. 75, no. 8, pp. 1063–1065, 1999.
- [22] K. Sarychev, D. A. Genov, A. Wei, and V. M. Shalaev, "Periodical arrays of optical nanoantennas," in *Proceedings of SPIE, Complex Mediums IV: Beyond Linear Isotropic Dielectrics*, Aug. 2003, pp. 165–168.
- [23] J. Li and N. Engheta, "Optical leaky-wave nano-antennas using plasmonic nanowires with periodical variation of permittivity," presented at the 2005 Annual Meeting of the Optical Society of America (OSA), Tucson, Arizona, Oct. 16–20, 2005.
- [24] J. Li, A. Salandrino, and N. Engheta, "Radiation characteristics and beam forming of multi-particles nanoantennas at optical frequencies," in *IEEE Int. Workshop on Antenna Technology (iWAT'06): Small Antennas and Novel Metamaterials*, White Plains, NY, Mar. 2006, pp. 432–433.
- [25] J. Li, A. Salandrino, and N. Engheta, "Shaping the beam of light in nanometer scale: A Yagi-Uda nanoantenna in optical domain [Online]. Available: <http://arxiv.org/abs/cond-mat/0703086>

- [26] P. B. Johnson and R. W. Christy, "Optical constants of the noble metals," *Phys. Rev. B*, vol. 6, no. 12, pp. 4370–4379, Dec. 1972.
- [27] A. L. Aden and M. Kerker, "Scattering of electromagnetic waves from two concentric spheres," *J. Appl. Phys.*, vol. 22, no. 10, pp. 1242–1246, Oct. 1951.
- [28] C. F. Bohren and D. R. Huffman, *Absorption and Scattering of Light by Small Particles*. New York: Wiley, 1983.
- [29] R. E. Collin, *Field Theory of Guided Waves*, ser. Electromagnetic Wave Theory, 2nd ed. New York: IEEE Press, 1991.
- [30] L. B. Felsen and N. Marcuvitz, *Radiation and Scattering of Waves*. Englewood Cliffs, NJ: Prentice-Hall, 1973.
- [31] R. R. Chance, A. Prock, and R. Silbey, "Molecular fluorescence and energy transfer near interfaces," in *Advances in Chemical Physics Volume XXXVII*, I. Prigogine and S. A. Rice, Eds. New York: Wiley, 1978, pp. 1–65.



Jingjing Li (S'07) received the B.S. degree in electrical engineering from Tsinghua University, Beijing, China, in 2000 and is currently working toward the Ph.D. degree in electrical engineering at the University of Pennsylvania, Philadelphia.

His dissertation work focuses on the design of optical antennas for communication and biology-inspired applications. His graduate research also covers nanophotonics, plasmonics, metamaterials, and nanoscale optomechanical resonating structures.



Nader Engheta (S'80–M'82–SM'89–F'96) received the B.S. degree from the University of Tehran, Iran, in 1978 and the M.S. and Ph.D. degrees from the California Institute of Technology (Caltech), in 1979 and 1982, respectively, all in electrical engineering.

After spending one year as a Postdoctoral Research Fellow at Caltech and four years as a Senior Research Scientist as Kaman Sciences Corporation's Dikewood Division in Santa Monica, CA, he joined the faculty of the University of Pennsylvania,

Philadelphia, in July 1987, where he is currently the H. Nedwill Ramsey Professor of Electrical and Systems Engineering and also holds an appointment in the Bioengineering Department. He is also a member of the David Mahoney

Institute of Neurological Sciences. He was the Graduate Group Chair of Electrical Engineering from July 1993 to June 1997. He is the co-editor of the book *Metamaterials: Physics and Engineering Explorations* (Wiley-IEEE Press, 2006). His current research interests and activities span over a broad range of areas including metamaterials and plasmonics, nanooptics and nanophotonics, nanocircuits and nanostructures modeling, bio-inspired/biomimetic polarization imaging and reverse engineering of polarization vision, miniaturized antennas and nanoantennas, hyperspectral sensing, biologically-based visualization and physics of sensing and display of polarization imagery, through-wall microwave imaging, millimeter-wave lensing systems, fractional operators and fractional paradigm in electrodynamics.

Dr. Engheta is a Guggenheim Fellow, a recipient of the IEEE Third Millennium Medal, and a Fellow of the Optical Society of America. He is a member of the American Physical Society (APS), the American Association for the Advancement of Science (AAAS), Sigma Xi, Commissions B, D, and K of the U.S. National Committee (USNC) of the International Union of Radio Science (URSI), and a member of the Electromagnetics Academy. He is the Vice-Chair/Chair-Elect of Commission B of USNC-URSI for 2006–2008. He has received various awards and distinctions for his scholarly research contributions and teaching activities including selection as one of the 2006 Scientific American 50 leaders in science and technology, the UPS Foundation Distinguished Educator Term Chair, the Fulbright Naples Chair award, and an NSF Presidential Young Investigator (PYI) award. He was twice awarded the S. Reid Warren, Jr. Award from UPenn's School of Engineering and Applied Science, and received the Christian F. and Mary R. Lindback Foundation Award, and the W. M. Keck Foundation's 1995 Engineering Teaching Excellence Award. He is an Associate Editor of the IEEE ANTENNAS AND WIRELESS PROPAGATION LETTERS (2002–present), and was an Associate Editor for the IEEE TRANSACTIONS ON ANTENNA AND PROPAGATION (1996–2001), and *Radio Science* (1991–1996). He was on the Editorial Board of the *Journal of Electromagnetic Waves and Applications*. He served as an IEEE Antennas and Propagation Society Distinguished Lecturer for the period 1997–99. He was the Chair (1989–91) and Vice-Chair (1988–89) of the joint chapter of the IEEE ANTENNAS AND PROPAGATION/MICROWAVE THEORY AND TECHNIQUES in the Philadelphia Section. He served as a member of the Administrative Committee (AdCom) of the IEEE Society of Antennas and Propagation from January 2003 till December 2005. He has been a Guest Editor/Co-Editor several special issues, namely, the special issue of the *Journal of Electromagnetic Waves and Applications* on the topic of "Wave Interaction with Chiral and Complex Media" in 1992, part special issue of the *Journal of the Franklin Institute* on the topic of "Antennas and Microwaves" (from the 13th Annual Benjamin Franklin Symposium) in 1995, the special issue of *Wave Motion* on the topic of "Electrodynamics in Complex Environments" in 2001, and the IEEE TRANSACTIONS ON ANTENNAS AND PROPAGATION *Special Issue on Metamaterials* in 2003.